Small field proton irradiation for in vivo studies: Potential and limitations when adapting clinical infrastructure

Monika Clausen ^{a,*}, Sirinya Ruangchan ^{a,b}, Arame Sotoudegan ^a, Andreas F. Resch ^a, Barbara Knäusl ^a, Hugo Palmans ^{c,d}, Dietmar Georg ^{a,c}

Received 12 May 2022; accepted 4 October 2022

Abstract

Purpose: To evaluate the dosimetric accuracy for small field proton irradiation relevant for pre-clinical in vivo studies using clinical infrastructure and technology. In this context additional beam collimation and range reduction was implemented.

Methods and materials: The clinical proton beam line employing pencil beam scanning (PBS) was adapted for the irradiation of small fields at shallow depths. Cylindrical collimators with apertures of 15, 12, 7 and 5 mm as well as two different range shifter types, placed at different distances relative to the target, were tested: a bolus range shifter (BRS) attached to the collimator and a clinical nozzle mounted range shifter (CRS) placed at a distance of 72 cm from the collimator. The Monte Carlo (MC) based dose calculation engine implemented in the clinical treatment planning system (TPS) was commissioned for these two additional hardware components. The study was conducted with a phantom and cylindrical target sizes between 2 and 25 mm in diameter following a dosimetric end-to-end test concept.

Results: The setup with the CRS provided a uniform dose distribution across the target. An agreement of better than 5% between the planned dose and the measurements was obtained for a target with 3 mm diameter (collimator 5 mm). A 2 mm difference between the collimator and the target diameter (target being 2 mm smaller than the collimator) sufficed to cover the whole target with the planned dose in the setup with CRS. Using the BRS setup (target 8 mm, collimator 12 mm) resulted in non-homogeneous dose distributions, with a dose discrepancy of up to 10% between the planned and measured doses.

Conclusion: The clinical proton infrastructure with adequate beam line adaptations and a state-of-the-art TPS based on MC dose calculations enables small animal irradiations with a high dosimetric precision and accuracy for target sizes down to 3 mm.

Keywords: Small field irradiation; Proton pencil beam scanning; Pre-clinical in vivo studies; Clinical infrastructure; Collimator; Dosimetry

E-mail: monika.clausen@meduniwien.ac.at (M. Clausen).

^a Division of Medical Radiation Physics, Department of Radiation Oncology, Medical University of Vienna, Austria

^b Division of Therapeutic Radiation and Oncology, Department of Radiology, King Chulalongkorn Memorial Hospital, Bangkok, Thailand

^c Division of Medical Physics, MedAustron Ion Therapy Center, Wiener Neustadt, Austria

^d National Physical Laboratory, Teddington, United Kingdom

^{*} Corresponding author: Monika Clausen, Division of Medical Radiation Physics, Department of Radiation Oncology, Medical University of Vienna, Austria

1 Introduction

Pre-clinical in vivo studies are essential components of basic and translational research in radiation oncology, e.g., to improve understanding of radiation effects in tissues, to test hypothesis or to develop multimodality treatments. For photon beam therapy, commercial solutions have been developed including high-precision small animal irradiators with image guidance that enable to mimic advanced photon therapy [1-3]. The situation is different for particle beams, mainly due to higher investment costs for particle accelerators. Although new approaches for small animal particle therapy emerge from laser-driven proton beam generation [4,5], most current experimental settings for pre-clinical in vivo studies are based on technology developed for clinical particle therapy [6-8]. This situation is expected to remain in the coming years.

Despite the increasing number of particle therapy facilities, the experience of performing pre-clinical studies with proton or carbon-ion beams is limited. The lack of dedicated small animal particle beam irradiators and the required adaptations of clinical beam lines might be the dominant factors. On the other hand, setting up a pre-clinical small animal irradiation solution based on recent technological advancements (e.g., commercially available Monte Carlo based dose calculation, scanned beam delivery) for clinical particle therapy does not require large additional investments (on top of the cost of an existing facility). Above all, the research outcome achieved in clinical beam lines might even be more representative from a translational research perspective. Disadvantages of utilizing a clinical beam line are the necessary adaptations to be able to irradiate very small volumes at shallow depths with high precision and accuracy in the presence of steep dose gradients. Pencil beam scanning (PBS) is becoming the most prevalent delivery method in particle therapy enabling a conformal target irradiation [9-11]. Proton pencil beam sizes are typically between 7 and 20 mm (full width at half maximum (FWHM)), with increasing diameter for lower energies. These dimensions are relatively large compared to target sizes in small animals (95% of all in vivo studies are conducted in mice [12]). Consequently, healthy tissue sparing is not optimal and passive beam shaping tools, such as collimators, are required. Attention should be given to neutron production and activation of the collimator and safe handling of the collimator by the user after irradiation experiments. A range shifter (RS) is needed since even the lowest proton energies, typically around 60 MeV in clinical beam lines, would position the Bragg peak at too large a depth in small animals. An overview of typical structures and organ sizes in small animals is given in the Supplementary material, Table A. Specific guidelines and recommendations for the welfare and use of animals in cancer research provide the maximal tumor sizes, where the

mean tumor diameter should not exceed 12 mm in mice and 25 mm in rats [12].

Besides beam delivery, a reliable treatment planning process including accurate dose calculation is a prerequisite for in vivo research. Again, for photon beam therapy, dedicated small animal treatment planning systems (TPS) have been developed and are commercially available [13,14], while for particle therapy no such solutions are available. The advantage of commercial solution comes along with an easy implementation of animal positioning (and coordinate transformation), image fusion, plan optimization as well as dose and linear energy transfer (LET) calculation. Such an infrastructure simplifies the workflow and macro- and micro dosimetric data acquisition significantly. Although pre-clinical in-vivo studies require a multidisciplinary setting, it can be expected that researchers of other professions than Medical Physics, e.g., biologist benefit from user friendly commercial systems in which treatment planning workflows are inherently implemented. In most particle beam therapy related pre-clinical studies, pre-defined structures were irradiated with monoenergetic beams, a scenario that does not reflect clinical reality [15-17]. The LET variations as an important factor concerning radiobiological effects cannot be efficiently studied in monoenergetic beams. Continuous developments and technological advancements in radiation oncology push the current boundaries, where MC based dose calculation is one prominent example. The availability of treatment planning systems with MC algorithms along with small calculation grids, adequate for proper visualization and delineation of small structures, will offer notable improvements.

In this study we report on a small field proton irradiation capability relevant for pre-clinical in vivo studies. Both dose delivery and dose calculation aspects are covered, with as main objective the determination of the lower field size limits for small volume irradiations, fulfilling the criteria of acceptable dose agreement of 5% between the planned and measured dose. The effects of beam collimation and energy degradation were investigated for cylindrical target sizes between 2 and 25 mm in diameter. Validation of a clinical TPS with MC based dose calculation for small field irradiation is performed and its limitations are revealed. Even though the results presented are center specific, the experimental setting and the related commissioning aspects are generally applicable for other centers aiming at small animal irradiations with clinical proton beams.

2 Materials and methods

2.1 Beam delivery

All investigations were performed in the research irradiation room of the synchrotron based clinical particle therapy center (MedAustron Ion Therapy Center, Wiener Neustadt,

Austria). The beamline and in-room equipment, such as robotic positioning table (BEC, Germany) and in-room imaging devices (MedPhoton, Austria), were tailored and commissioned comparable to the clinical irradiation rooms [13].

Protons were delivered with a fixed horizontal beamline in the form of narrow beams with lateral spot sizes of 7 mm (FWHM) for the highest nominal beam energy (252.7 MeV) and 21 mm for the lowest beam energy (62.4 MeV). The beams were scanned laterally across the field by fast-scanning magnets (using the pencil beam scanning dose delivery technique) and the beam energies were varied by active energy modulation directly in the synchrotron [18,19].

Several adaptations of the beam line were necessary to irradiate small targets. The lowest available nominal proton energy is 62.4 MeV, corresponding to a range of 30 mm in water. For shallow target depths, typical in small animals, two different types of range shifter (RS) were tested for energy degradation, placing their scatter contributions at two distances relative to the phantom. The bolus RS (BRS) was attached directly to the phantom in the form of a PMMA (Polymethyl Methacrylate) block with a water equivalent thickness (WET) of 2.4 cm. Beam energies for the setup with BRS varied between 62.4 MeV and 76.9 MeV. The second type was the clinical, nozzle-mounted RS (CRS) with a WET of 3.5 cm. The CRS was inserted into the beam path at the end of the beamline at a distance of 72 cm from the phantom's surface. The typical energy range in the setup with the CRS was between 72.4 MeV and 86.4 MeV.

Another essential beam line adaptation consisted of a collimator. The range shifter modulated pencil beams are large compared to target sizes of less than 3 cm. In practice, that means that without using a collimator a substantial part of the animal outside of the target volume would be covered with a dose similar to the target dose. The collimators used in this study were made of brass with a thickness of 10 mm (corresponding to about 5 cm WET) and with cylindrical apertures of 15, 11, 7 or 5 mm in diameter.

2.2 Dose calculations

All dose calculations for small fields were performed in the commercial TPS RayStation v7.99.3 (RaySearch Laboratories, Sweden) developed for clinical applications. The beam model was validated by dose verification measurements in isocentric as well as non-isocentric conditions according to clinical requirements [20] with a total uncertainty of 3% (1 Standard Deviation) for MC based dose calculations (clinical MC dose engine v4.3).

2.3 Phantom

The block shaped phantom, representing in its size a small animal, consisted of water equivalent Gammex-457

CTG (Sun Nuclear, USA) material with a density of 1.04 g cm⁻³ and PMMA with a density of 1.19 g cm⁻³. The cylindrically shaped target (Gammex) with a diameter of 25 mm and length of 15 mm was surrounded by PMMA. Individual slabs with an area of 40 × 40 mm² and a thickness of 5 mm were assembled to form the phantom. The first slab of the phantom consisted of PMMA only and the target started at a depth of 5 mm. Slicing of the phantom was a practical solution allowing detector insertion at various discrete depths. Furthermore, the individual slabs could be combined to allow for different setups, i.e., with the BRS or CRS. The phantom was positioned with its surface close to the isocenter at a distance of about 70 cm from the nozzle. In one of the two RS setups, the BRS was positioned directly in front of the phantom.

2.4 Treatment planning

The computed tomography (CT) dataset of the phantom was acquired with a microCT system (X-cube, Molecubes, Germany), dedicated to small animal imaging with a resolution of 200 µm and tube voltage of 50 kV. The 3D volumetric data set from the microCT system was subsequently converted into sliced format with the 3D slicer software (https://www.slicer.org) and the DICOM header was modified to allow import into the clinical TPS. The same image set was used for treatment plan creation and dose calculation for all tested scenarios. The material properties were overwritten in the TPS with the known properties of the phantom materials (density and material compositions). A schematic representation of the setup with the phantom and corresponding overwritten materials (collimator, CRS, BRS, target) is shown in Fig. 1. Small targets with various diameters (25 mm down to 2 mm) and a constant thickness of 15 mm were delineated with a resolution of 1 mm concentrically within the Gammex material.

Every irradiation field was optimized in the TPS to deliver a prescribed physical dose of 1 Gy to the target. All treatment plan optimizations and dose calculations were solely based on the MC algorithm. The the smallest possible $(1 \times 1 \times 1 \text{ mm}^3)$ dose calculation grid size, optimized with 10^5 particles per spot and a tolerance of 0.5% on the relative type-A uncertainty (1SD) of the dose in each target voxel was applied in the final dose calculation. A combination of parameters, including a spot distance of 1 mm or 2 mm, which are standard settings for patient treatments to achieve uniform lateral dose distributions, was tested to find an optimal solution for the predicted dose distribution.

Both the RSs and collimators were modelled in the TPS. The BRS was represented by an extra slab of PMMA added in front of the phantom. The CRS could be selected in the TPS as an external element. For the dose calculations with

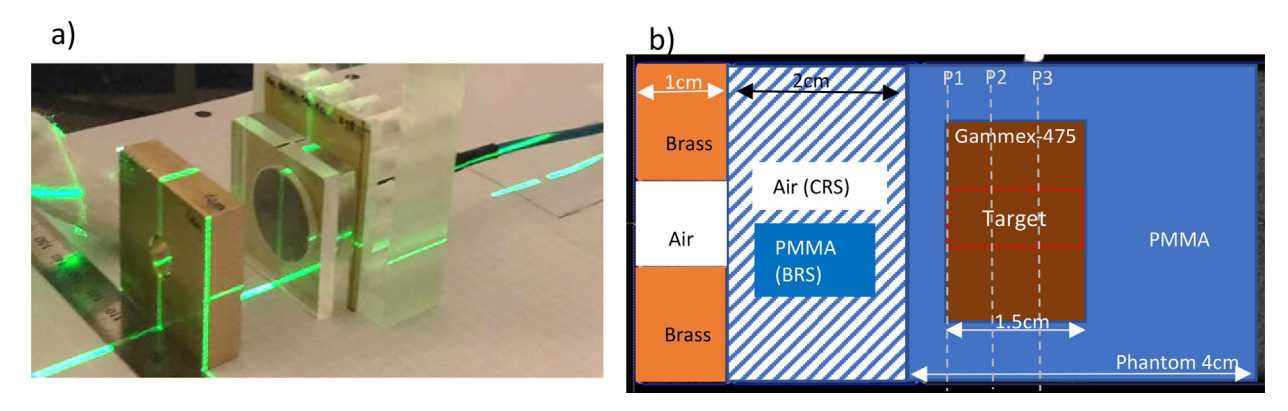


Figure 1. Experimental setup with a collimator. a) The stack of three films is placed in the second measurement position (P2). The microDiamond detector is inserted into the holder and placed just behind the films. b) Schematic representation of the experimental setup. The collimator (brass), bolus BRS (PMMA) or air (for CRS), phantom and target (red dotted rectangle) were delineated and overwritten in the TPS with the corresponding materials. The measurement positions (for EBT3 films and microDiamond detector) are labeled for the proximal position with P1 and for SOBP positions with P2 and P3. They are indicated in the figure with the grey dashed lines. The beam is coming from the left.

CRS, the BRS in the microCT scan was overwritten in the TPS by air (Fig. 1).

The collimator was simulated in the TPS by delineating and overwriting the proximal part of the microCT scan of the setup by brass material, leaving out the cylindrical opening of the respective collimator size, which was overwritten by air. Additionally, open fields without collimator in the beam line were simulated and measured.

2.5 Dose verification

Dose delivery verification was performed with two detectors: the microDiamond (PTW-60019, PTW, Germany) and EBT3 radiochromic film (Gafchromic TM, USA). The active volume of the microDiamond detector (0.004 mm³) has a circular diameter of 2.2 mm and thickness of 1 µm. The detector was cross-calibrated against a Roos-type ionization chamber (PTW-34001, PTW, Germany), which was calibrated in terms of absorbed dose to water in a Co-60 beam traceable to the German primary standard of absorbed dose [21]. EBT3 films were chosen for measurements of lateral dose distributions due to their high spatial resolution and tissue equivalency. Three film sheets of $5 \times 4 \text{ cm}^2$, each with a thickness of 278 µm (WET 0.358 µm), were stacked together and inserted at three different depths (P1, P2, P3, see Fig. 1b) of the target. The proximal position P1 was at the beginning of the target and measurement positions P2 and P3 at 5 mm and 10 mm depth within the target, respectively. Due to the limited beam time only the positions within the spread-out Bragg Peak (SOBP) (P2, P3) were investigated for some setups. The final reported dose value and the corresponding uncertainty at each position was an

average of lateral line profiles from three films with its estimated standard deviation. To account for the non-linearity of the net optical density of the films as a function of absorbed dose to water, films were calibrated against the Advanced Markus ionization chamber (PTW-34045, PTW, Germany). The corresponding calibration curve was obtained at 2 cm depth in water, at a nominal proton energy of 179 MeV and for a dose range of 0.25–12 Gy. The film handling and evaluation is described in more detail in [22].

Signal quenching due to the beam energy dependence of radiochromic films was experimentally determined at each measurement depth (position) by comparison with the microDiamond measurements. A plan to irradiate the target of 2.5 cm (without any collimator) was created in the TPS for the same energy range as the setup with the clinical range shifter. Dosimetric measurements (without collimator) were performed with either 3 films or the microDiamond detector at 3 positions within the phantom (P1, P2, P3). The response of cross-calibrated EBT3 films was compared to microDiamond response to determine quenching corrections. By doing so factors of 1.04 were obtained for positions P1 and P2 and 1.06 for position P3. These factors were subsequently applied for films in all other setups, respectively.

To increase the beam time efficiency and reduce the measurement time, the microDiamond detector in a face-on orientation was typically placed right behind the three films and irradiated simultaneously such that the flat face of the microDiamond encapsulation was aligned behind the films with positions P1, P2, P3 (such that the sensitive diamond layer of the detector was 1.5 mm deeper than the start of the target). The setup with the collimator where the films and microDiamond detector were irradiated at the second

Table 1
Summary of parameters and settings of all investigated setups. The clinical range shifter is used in the setup (unless stated otherwise). The reported dose values for EBT3 films (and corresponding standard uncertainties) are determined from an average of lateral line profiles (within the defined target size) of three films. The microDiamond detector provides the point dose at the center of the field. The standard deviations of the microDiamond measurements were smaller than the number of reported digits and are therefore not reported. The values in brackets represent the corresponding dose values from the TPS.

Target size [mm]	Coll. size/dist. to phantom [mm]	TPS modelling of collimator	Dose at P1 (proximal target) [Gy]		Dose at P2, P3 (SOBP) [Gy]	
			EBT3 (TPS)	micro Diamond (TPS)	EBT3 (TPS)	micro Diamond (TPS)
25	11/40	no	$1.10 \pm 0.10 \ (1.00)$	1.14 (1.00)	$1.11 \pm 0.11 \ (1.01)$	1.10 (1.02)
12	_	no	$1.05 \pm 0.03 \; (0.98)$	1.05 (1.00)	$1.04 \pm 0.02 \ (1.02)$	1.07 (1.02)
12	15/20	yes	$1.02 \pm 0.08 \; (1.01)$	1.03 (1.00)	$1.00 \pm 0.01 \ (1.02)$	1.03 (1.02)
12	15/20	yes	$(0.92)^{BRS}$	1.09 (1.00) BRS	$1.04 \pm 0.08 (0.96)^{BRS}$	1.04 (1.09) BRS
8	11/20*/**	yes	_	_	$0.98 \pm 0.03*/0.81 \pm 0.39^{**}$	_
8	11/20	yes	$0.98 \pm 0.01 \; (0.99)$	(0.99)	$0.99 \pm 0.01 \ (1.00)$	(1.00)
8	11/20	no	1.01 ± 0.02	_	0.97 ± 0.02	1.01
8	11/40	no	1.06 ± 0.02	_	1.02 ± 0.02	1.02
5	7/20	yes	$0.93 \pm 0.01 \; (0.99)$	0.96 (0.95)	$0.97 \pm 0.01 \ (1.00)$	1.05 (0.99)
4	7/20	yes	$0.87 \pm 0.01 \; (0.98)$	(0.95)	$0.98 \pm 0.04 \; (1.00)$	1.03 (1.00)
4	5/20	yes	$0.86 \pm 0.02 \; (0.94)$	0.96 (0.98)	$1.08 \pm 0.06 \ (1.02)$	1.23 (1.16)
3	7/20	yes	$0.88 \pm 0.01 \; (1.03)$	(0.98)	$0.98 \pm 0.01 \; (1.01)$	1.04 (1.00)
3	5/20	yes	$0.88 \pm 0.01 \; (1.01)$	0.95 (0.98)	$1.02 \pm 0.02 \ (1.02)$	1.09 (1.04)
2	5/20	yes	$0.84 \pm 0.01 \; (0.96)$	0.91 (0.94)	$0.98 \pm 0.03 \; (0.93)$	1.04 (1.01)

BRS Bolus range shifter.

measurement position (P2) is shown in Fig. 1a). The type-A uncertainty assessment for the microDiamond detector was performed without films, with repetitive measurements where the detector was placed at one measurement position and irradiated with the same field three times.

The impact of collimator misalignment and the propagation of the collimator position accuracy on the target dose distribution were quantified with the setup using the CRS. The collimator was either well aligned with the phantom (centered) or shifted by 1 mm and 2 mm in both horizontal directions. In total 15 different configurations were used with different targets, collimators and other relevant settings, an overview of which is provided in Table 1. In general, only minor differences were observed in lateral profiles between position P2 and P3 (both in SOBP). The averaged values of these two positions obtained from detectors are listed in Table 1. Larger discrepancies were observed for position P1, especially for smaller targets (< 5 mm), as discussed in Section 3.3.

In addition to measurements, independent dose calculations were carried out for some measurement scenarios using Gate/Geant4 simulations [23,24]. In the simulations the exact experimental setup was modeled tracking all particles through the nozzle elements using a validated beam model

[19]. The simulation settings were identical to those reported in an earlier study [25].

3 Results

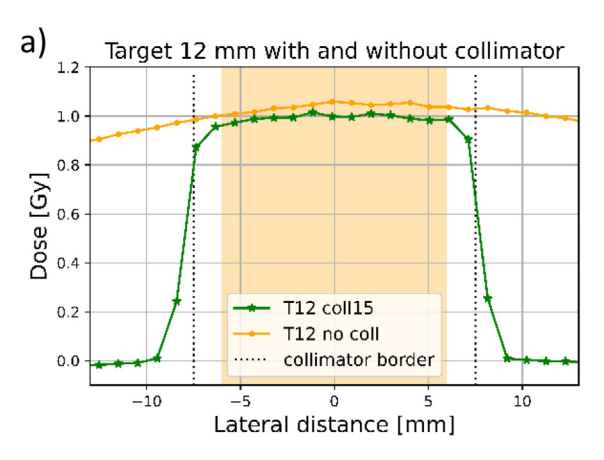
3.1 Beam collimation

Fig. 2a demonstrates the importance of beam collimation for small field irradiation; in the setup without a collimator (neither planned in TPS nor included in the setup), a dose of more than $0.5 \, \text{Gy}$ covered the whole phantom area $(40 \times 40 \, \text{mm}^2)$ laterally. The dose distribution in the target was non-uniform and exceeded the planned dose by up to 7% (as measured with the microDiamond) at the center of the target. The setup with the collimator (planned in TPS for calculation) resulted in a homogeneous target dose distribution agreeing within 1.5% with the planned dose (1 Gy). The lateral penumbra (R80/R20) was 1 mm in this setup.

The results of the approach where a treatment plan was designed for a target of 8 mm and a collimator of 11 mm was placed in front of the phantom (which was not included for the dose calculation in the TPS) are shown in Fig. 2b (blue and orange profiles). Two different distances between the collimator and phantom (40 mm and 20 mm)

^{*} Collimator with 1 mm horizontal misplacement.

^{**} Collimator with 2 mm horizontal misplacement.



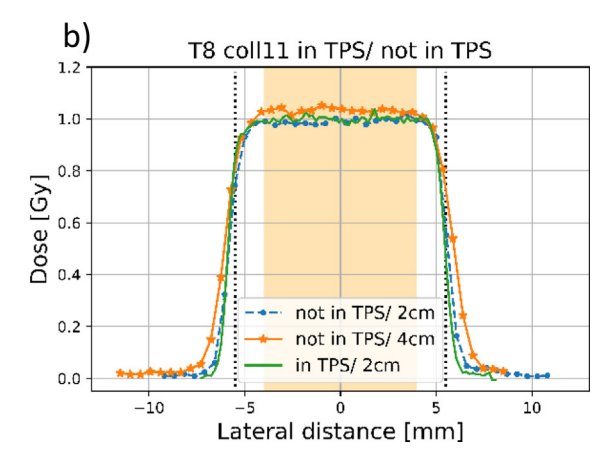


Figure 2. Lateral dose profiles (EBT3) in position P2 in the setups with CRS; a) for the target of 12 mm (T12) for the setup with and without the collimator and b) for the target of 8 mm (T8) and collimator with 11 mm opening either modelled (included) in TPS (green line) or not modelled (orange and blue markers) in the TPS. The shaded area indicates the target dimension, while the black dotted vertical lines show the collimator openings.

were investigated. The results were comparable to those obtained with the approach where the collimator was modelled in the TPS (also shown in Fig. 2b by the green profile). Larger discrepancies between the planned and measured dose were observed when the target size was larger than the collimator opening (data shown in Table 1). In general, dose calculation errors exceeded the limit of 5% for targets larger than 1.5 cm at shallow depths of less than 1 cm in combination with the CRS for both scenarios (with or without the collimator).

The collimator misalignment was systematically tested in the setup with the CRS and a target size of 12 mm (collimator 15 mm). The averaged dose of 0.98 Gy was well within the limits for the collimator shift of 1 mm. The shift of 2 mm led to a significant underdosage compared to central alignments with an averaged target dose of 0.81 Gy. The line dose profiles obtained from the irradiated films with a colli-

mator shift of 2 mm and those for the central alignment are given in Supplementary material, Figure Ba).

3.2 Range reduction

Achieving a homogenous dose distribution in the TPS was more challenging with the BRS when comparing the two types of RS. The differences between the optimized dose distributions for the BRS and CRS setups were in agreement with those from independent dose calculations (Gate/Geant4) and also confirmed by the measurements. The dose distribution in the target with the CRS was homogeneous and the lateral penumbra of 1 mm was smaller compared to the penumbra of 2 mm for the setup with the BRS. Examples of lateral dose profiles acquired at the second measurement position, from the Gate/Geant4 simulations, TPS predictions and measurements with EBT3 films are

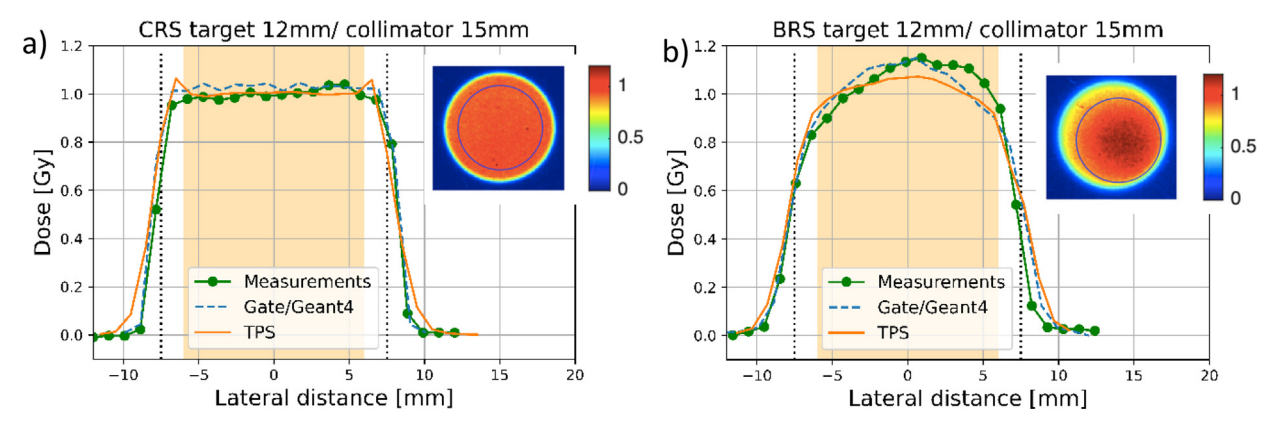


Figure 3. Lateral dose profiles (EBT3) at measurement position P2 (10 mm depth), a) for the setup with the CRS and b) for the setup with the BRS. Measurements with EBT3 films are compared with TPS and Gate/Geant4 calculations. The corresponding color map distributions are also shown. The circles in the color maps indicate the target sizes and the area in which the dose was evaluated. The shaded area indicates the target dimension while the black dotted vertical lines show the collimator opening.

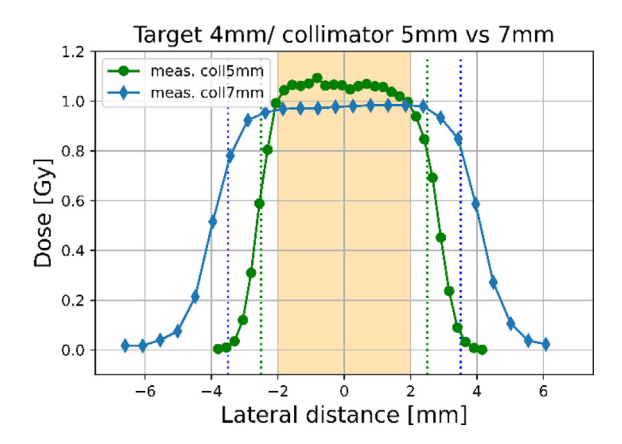


Figure 4. Lateral dose profiles (EBT3) in SOBP at measurement position P2 for target size of 4 mm with collimator openings of 5 and 7 mm. The shaded area indicates the target dimension, while the dotted vertical lines indicate the collimator openings.

shown in Fig. 3. In repeated measurements it was observed that the setup with BRS was more prone to setup errors than the setup with the CRS and even a small collimator misalignment of less than 1 mm resulted in a pronounced asymmetry in the dose distribution within the target (color map distribution in Fig. 3b)). It is worth mentioning that improved dose distributions with BRS, i.e., with more homogeneous distribution across the target, were obtained at smaller distances to the nozzle exit window (data not provided) even though the penumbra remained larger compared to the CRS. Because the setup for the final animal irradiation requires a certain airgap between the nozzle and the collimator (> 50 cm), the majority of investigations in this study were continued with the CRS.

3.3 Field size and target coverage

Various field sizes in combination with different collimators were investigated in order to find a minimal difference between the collimator opening with respect to the target. Fig. 4 compares dose distributions in the SOBP (average of P2, P3) for the target size of 4 mm and two different collimators: 5 and 7 mm. A difference of 1 mm between the aperture size (5 mm) and target size (4 mm) led to a dose overestimation in TPS. For all tested target sizes, it was found that a minimum of 2 mm between the aperture and target size (target size being 2 mm smaller than the aperture) was needed to cover the target with the prescribed dose. From all investigated setups, the larger differences did not provide systematic improvements in target dose distributions. Table 1 summarizes the dosimetric results for all target sizes and the respective collimator/ distance settings.

The dose could not be predicted within 5% by the TPS for the collimators smaller than 7 mm at the first measure-

ment position (P1), just before the SOBP. The dose in this part of the target acquired with EBT3 films systematically decreased with smaller collimator diameter (Supplementary material, Figure Bb). This might be attributed partially to the broader beam distribution and larger scatter of low energy protons contributing to the proximal target coverage. Moreover, potentially higher LET contributions from low energy protons can lead to pronounced signal quenching in films. It is important to note that this discrepancy was smaller between the microDiamond detector and TPS predictions. The effective point of measurement of the detector was positioned 1.5 mm deeper in the target (compared to films because of the setup of the microDiamond behind three films) and the agreement between the measurements and TPS prediction was better at this depth.

4 Discussion

The purpose of this study was to investigate the feasibility and accuracy of small field irradiation with proton beams using clinical infrastructure. Target sizes ranging from 25 mm down to 2 mm were investigated from a dosimetric point of view for in vivo radiobiological research. The results demonstrate, on the one hand, the feasibility of using the clinical proton treatment infrastructure for small field high-precision and accurate pre-clinical small animal irradiation, but underlines, on the other hand, the necessity of beamline modifications. By doing so, acceptable dosimetric agreement of better than 5 % between planning and measurements was achieved in the target (within the SOBP) for target sizes down to 3 mm for both detectors used, i.e., the microDiamond and EBT3 films. The results can be transferred to other centers equipped with pencil beam scanning technology and Monte Carlo based dose calculation engines, leading to comparable dosimetric accuracy when using range shifters and collimators in a similar experimental arrangement for small field irradiation.

Until now, available commercial TPSs were not recommended for small field irradiation due to the potentially limited accuracy of the calculation of dose and lateral field penumbrae [26]. Previous studies pointed out the limitation of analytical dose calculations at tissue interfaces of different tissue densities and complex anatomic geometries [27,28]. The analytical approach tested in the frame of this study (data not provided) resulted in a poor target coverage and unacceptable dose distributions when a collimator was included in the dose calculations. The recent implementation of MC based dose calculation solutions for proton beams, however, significantly improves the dose calculation accuracy for small targets. Tailored solutions for clinical or pre-clinical applications e.g., delineation accuracy adapted to the high resolution of microCT scan and smaller dose calculation grid size, as well as the inclusion of collimator, will continuously improve the treatment and research outcome in the future.

Up to 6% higher doses were observed for the small field irradiation using the CRS without a collimator. This overdose was, however, not observed with the collimator. This might be explained by secondary particle production and their modelling in the TPS. Secondary particles, which are generally not accurately modeled in dose calculations algorithms, are shielded when using collimators and therefore contribute less to systematic dose uncertainties. In other words, without a collimator a wide scatter field can contribute substantially to the target dose [20] and thus explain the observed dose deviations between measurements and calculations for small fields. Therefore, besides the healthy tissue and critical structure avoidance, the collimation can also improve dose calculation accuracy for small fields relevant to small-animal research.

Investigations of minimal collimator openings led to the conclusion that a two-millimeter difference between the collimator and the target (target being 2 mm smaller than the collimator) suffices to deliver the prescribed dose covering the whole target in the CRS setup. Equal target and collimator sizes led to constraints that could not be met in dose calculations already at the treatment planning stage of the irradiation workflow.

The limitations of the TPS with respect to dose calculation accuracy were reached at the proximal part of the target, i.e., dose coverage decreased with decreasing collimator diameter and target size at the proximal target depth. These differences might be related to broader beam distribution and larger scatter of low energy protons contributing to the proximal target coverage. This uncertainty can be reduced by applying target margins for in vivo irradiation studies, which was not applied in this purely dosimetric investigation. An opposite observation with higher target dose was reported for small proton fields for ocular treatments [29]. The latter study, however, reports measurements in a different setup with a double scattering system and a different optimization strategy that does not include patient specific weighting of range modulation.

The relatively large distance of 72 cm between the CRS and the collimator, as used in typical patient treatment configurations, provided a uniform dose distribution across the target, whereas the BRS solution resulted in a non-uniform peak-shaped distribution. The BRS setup was in addition very sensitive to misalignment errors whereas the setup with the CRS tolerated slight lateral collimator misplacements of about 1 mm. This is in line with the study from Ciocca et al. [30], where a comparison of different CRS locations, relative to target, was performed in the scope of beamline adaptations for ocular treatments. Maximizing the air gap between CRS and

collimator increased the transversal dose homogeneity in the target and decreased the lateral dose fall-off distance.

Challenges in small field dosimetry arise from the current availability of appropriate detectors. Even though both detectors used in this study have certain drawbacks, a combination of a microDiamond detector and EBT3 films proved to be adequate for small proton field dosimetry within the target. The energy dependence of EBT3 films requires proper film calibration and corrections for signal quenching due to beam quality variation. MicroDiamond detector is a suitable candidate for accurate absolute dose determination in proton beams [31], which was confirmed also for small fields in the frame of this study with additional measurements and performance comparison of microDiamond against the Advanced Markus ionization chamber (PTW, Freiburg) (data not reported). The disadvantage of a single detector provides, however, only a point dose and requires measuring in many points increasing the measurement time especially in (energy-modulated) scanned beams.

Particle therapy centers aiming for pre-clinical studies will need, besides adaptations of their clinical infrastructure, clear guidelines for dose delivery and quality assurance to ensure the accuracy and reproducibility of research, which are still missing. Currently, it is recommended to follow as close as possible the guidelines for patient treatment [26] and involve the dosimetry physicists into the radiobiological research [32]. These recommendations were closely followed in this work.

Regarding several other steps of the treatment planning and irradiation workflow in pre-clinical research, a clinical planning CT reaches its limits in terms of resolution and image quality for small structures. Dedicated imaging systems are therefore preferable, such as a microCT. The microCT utilized in the present study to scan the phantom provided excellent image quality at a resolution of 200 μ m, which was five times higher than the typical clinical CT used for treatment planning. Higher image quality comes at a cost of increased imaging doses which are about an order of magnitude higher for the microCT than for a clinical CT. This is an important contribution and has to be considered in pre-clinical studies as it might alter the observed dose response relationship [33].

5 Conclusion

An adapted clinical PBS beam line in combination with state-of-the-art treatment planning system and MC based dose calculations, provides adequate dosimetric accuracy for small animal studies with proton beams for target sizes down to 3 mm.

Declaration of Competing Interest

The authors declare that they have no known competing financial interests or personal relationships that could have appeared to influence the work reported in this paper.

Acknowledgment

Sirinya Ruangchan gratefully acknowledges the financial support by PhD research grant from the Thai Red Cross Society, King Chulalongkorn Memorial Hospital, Bangkok.

Appendix A Supplementary material

Supplementary data to this article can be found online at https://doi.org/10.1016/j.zemedi.2022.10.002.

References

- [1] Stojadinovic S, Low DA, Hope AJ, Vicic M, Deasy JO, Cui J, et al. MicroRT-Small animal conformal irradiator. Med Phys 2007;34:4706–4716. https://doi.org/10.1118/1.2799887.
- [2] Verhaegen F, Granton P, Tryggestad E. Small animal radiotherapy research platforms. Phys Med Biol 2011;56:R55–R83. https://doi.org/10.1088/0031-9155/56/12/R01.
- [3] Treibel F, Nguyen M, Ahmed M, Dombrowsky A, Wilkens JJ, Combs SE, et al. Establishment of Microbeam Radiation Therapy at a Small-Animal Irradiator. Int J Radiat Oncol 2021;109:626–636. https://doi.org/10.1016/j.ijrobp.2020.09.039.
- [4] Bayart E, Flacco A, Delmas O, Pommarel L, Levy D, Cavallone M, et al. Fast dose fractionation using ultra-short laser accelerated proton pulses can increase cancer cell mortality, which relies on functional PARP1 protein. Sci Rep 2019;9:10132. https://doi.org/10.1038/s41598-019-46512-1.
- [5] Chaudhary P, Milluzzo G, Ahmed H, Odlozilik B, McMurray A, Prise KM, et al. Radiobiology Experiments With Ultra-high Dose Rate Laser-Driven Protons: Methodology and State-of-the-Art. Front Phys 2021:9. https://doi.org/10.3389/fphy.2021.624963.
- [6] Ford E, Emery R, Huff D, Narayanan M, Schwartz J, Cao N, et al. An image-guided precision proton radiation platform for preclinical in vivo research. Phys Med Biol 2017;62:43–58. https://doi.org/10.1088/1361-6560/62/1/43.
- [7] Patriarca A, Fouillade C, Auger M, Martin F, Pouzoulet F, Nauraye C, et al. Experimental Set-up for FLASH Proton Irradiation of Small Animals Using a Clinical System. Int J Radiat Oncol 2018;102:619–626. https://doi.org/10.1016/j.ijrobp.2018.06.403.
- [8] Parodi K, Assmann W, Belka C, Bortfeldt J, Clevert D-A, Dedes G, et al. Towards a novel small animal proton irradiation platform: the SIRMIO project. Acta Oncol (Madr) 2019;58:1470–1475. https://doi.org/10.1080/0284186X.2019.1630752.
- [9] Pedroni E, Enge H. Beam optics design of compact gantry for proton therapy. Med Biol Eng Comput 1995;33:271–277. https://doi.org/10.1007/BF02510499.
- [10] Lomax AJ, Böhringer T, Bolsi A, Coray D, Emert F, Goitein G, et al. Treatment planning and verification of proton therapy using spot scanning: Initial experiences. Med Phys 2004;31:3150–3157. https://doi.org/10.1118/1.1779371.
- [11] Paganetti H, Beltran C, Both S, Dong L, Flanz J, Furutani K, et al. Roadmap: proton therapy physics and biology. Phys Med Biol 2021;66:05RM01. https://doi.org/10.1088/1361-6560/abcd16.

- [12] Workman P, Aboagye EO, Balkwill F, Balmain A, Bruder G, Chaplin DJ, et al. Guidelines for the welfare and use of animals in cancer research. Br J Cancer 2010;102:1555–1577. https://doi.org/10.1038/sj.bjc.6605642.
- [13] Verhaegen F, van Hoof S, Granton PV, Trani D. A review of treatment planning for precision image-guided photon beam preclinical animal radiation studies. Z Med Phys 2014;24:323–334. https://doi.org/10.1016/j.zemedi.2014.02.004.
- [14] Chiavassa S, Nilsson R, Clément-Colmou K, Potiron V, Delpon G, Traneus E. Validation of the analytical irradiator model and Monte Carlo dose engine in the small animal irradiation treatment planning system μ -RayStation 8B. Phys Med Biol 2020;65:035006. https://doi.org/10.1088/1361-6560/ab6155.
- [15] van Hoof SJ, Granton PV, Verhaegen F. Development and validation of a treatment planning system for small animal radiotherapy: SmART-Plan. Radiother Oncol 2013;109:361–366. https://doi.org/10.1016/j.radonc.2013.10.003.
- [16] Biglin ER, Price GJ, Chadwick AL, Aitkenhead AH, Williams KJ, Kirkby KJ. Preclinical dosimetry: Exploring the use of small animal phantoms. Radiat Oncol 2019;14:1–11. https://doi.org/10.1186/s13014-019-1343-8.
- [17] Silvestre Patallo I, Subiel A, Westhorpe A, Gouldstone C, Tulk A, Sharma RA, et al. Development and Implementation of an End-To-End Test for Absolute Dose Verification of Small Animal Preclinical Irradiation Research Platforms. Int J Radiat Oncol 2020;107:587–596. https://doi.org/10.1016/j.ijrobp.2020.03.001.
- [18] Stock M, Georg D, Ableitinger A, Zechner A, Utz A, Mumot M, et al. The technological basis for adaptive ion beam therapy at MedAustron: Status and outlook. Z Med Phys 2017. https://doi.org/10.1016/j.zemedi.2017.09.007.
- [19] Elia A, Resch AF, Carlino A, Böhlen TT, Fuchs H, Palmans H, et al. A GATE/Geant4 beam model for the MedAustron non-isocentric proton treatment plans quality assurance. Phys Medica 2020;71:115–123. https://doi.org/10.1016/j.ejmp.2020.02.006.
- [20] Carlino A, Böhlen T, Vatnitsky S, Grevillot L, Osorio J, Dreindl R, et al. Commissioning of pencil beam and Monte Carlo dose engines for non-isocentric treatments in scanned proton beam therapy. Phys Med Biol 2019;64:17NT01. https://doi.org/10.1088/1361-6560/ab3557.
- [21] Osorio J, Dreindl R, Grevillot L, Letellier V, Kuess P, Carlino A, et al. Beam monitor calibration of a synchrotron-based scanned lightion beam delivery system. Z Med Phys 2021;31:154–165. https://doi.org/10.1016/j.zemedi.2020.06.005.
- [22] Khachonkham S, Dreindl R, Heilemann G, Lechner W, Fuchs H, Palmans H, et al. Characteristic of EBT-XD and EBT3 radiochromic film dosimetry for photon and proton beams. Phys Med Biol 2018. https://doi.org/10.1088/1361-6560/aab1ee.
- [23] Bagulya A, Brown JMC, Burkhardt H, Grichine V, Guatelli S, Incerti S, et al. Recent progress of GEANT4 electromagnetic physics for LHC and other applications. J Phys Conf Ser 2017;898:042032. https://doi.org/10.1088/1742-6596/898/4/042032.
- [24] Sarrut D, Bardiès M, Boussion N, Freud N, Jan S, Létang J-M, et al. A review of the use and potential of the GATE Monte Carlo simulation code for radiation therapy and dosimetry applications. Med Phys 2014;41:064301. https://doi.org/10.1118/1.4871617.
- [25] Resch AF, Elia A, Fuchs H, Carlino A, Palmans H, Stock M, et al. Evaluation of electromagnetic and nuclear scattering models in GATE/Geant4 for proton therapy. Med Phys 2019. https://doi.org/10.1002/mp.13472.
- [26] Verhaegen F, Dubois L, Gianolini S, Hill MA, Karger CP, Lauber K, et al. ESTRO ACROP: Technology for precision small animal radiotherapy research: Optimal use and challenges. Radiother Oncol 2018;126:471–478. https://doi.org/10.1016/j.radonc.2017.11.016.

- [27] Maes D, Saini J, Zeng J, Rengan R, Wong T, Bowen SR. Advanced proton beam dosimetry part II: Monte Carlo vs. pencil beam-based planning for lung cancer. Transl Lung Cancer Res 2018;7:114–121. https://doi.org/10.21037/tlcr.2018.04.04.
- [28] Ruangchan S, Knäusl B, Fuchs H, Georg D, Clausen M. Physica Medica Experimental benchmarking of RayStation proton dose calculation algorithms inside and outside the target region in heterogeneous phantom geometries. Phys Medica 2020;76:182–193. https://doi.org/10.1016/j.ejmp.2020.07.010.
- [29] Kacperek A. Protontherapy of eye tumours in the UK: A review of treatment at Clatterbridge. Appl Radiat Isot 2009;67:378–386. https://doi.org/10.1016/j.apradiso.2008.06.012.
- [30] Ciocca M, Magro G, Mastella E, Mairani A, Mirandola A, Molinelli S, et al. Design and commissioning of the non-dedicated scanning proton beamline for ocular treatment at the synchrotron-based

- <scp>CNAO</scp> facility. Med Phys 2019;46:1852–1862. https://doi.org/10.1002/mp.13389.
- [31] Gomà C, Marinelli M, Safai S, Verona-Rinati G, Würfel J. The role of a microDiamond detector in the dosimetry of proton pencil beams. Z Med Phys 2016;26:88–94. https://doi.org/10.1016/j.zemedi.2015.08.003.
- [32] Durante M, Paganetti H, Pompos A, Kry SF, Wu X, Grosshans DR. Report of a National Cancer Institute special panel: Characterization of the physical parameters of particle beams for biological research. Med Phys 2019:46. https://doi.org/10.1002/mp.13324.
- [33] Willekens I, Buls N, Lahoutte T, Baeyens L, Vanhove C, Caveliers V, et al. Evaluation of the radiation dose in micro-CT with optimization of the scan protocol. Contrast Media Mol Imaging 2010;5:201–207. https://doi.org/10.1002/cmmi.394.

Available online at: www.sciencedirect.com

ScienceDirect